rhythms and burst firing to tonic firing of both TRN and relay cells (29). Thus, mGluRs may play a role in regulating the spatial and temporal coordination of inhibition to the dorsal thalamus.

References and Notes

1. C. E. Landisman et al., J. Neurosci. 22, 1002 (2002).
2. M. A. Long, C. E. Landisman, B. W. Connors, J. Neurosci. 24, 341 (2004).
3. S. M. Sherman, C. Koch, Exp. Brain Res. 63, 1 (1986).
4. D. A. McCormick, M. von Krosigk, Proc. Natl. Acad. Sci. U.S.A. 89, 2774 (1992).
5. S. A. Eaton, T. E. Salt, Neuroscience 73, 1 (1996).
6. P. Golshani, R. A. Warren, E. G. Jones, J. Neurophysiol. 80, 143 (1998).
7. M. von Krosigk, J. E. Monckton, P. B. Reiner, D. A. McCormick, Neuroscience 91, 7 (1999).
8. M. V. Bennett, Ann. N. Y. Acad. Sci. 137, 509 (1966).
9. Y. Amitai et al., J. Neurosci. 22, 4142 (2002).
10. M. Galarreta, S. Hestrin, Nat. Rev. Neurosci. 2, 425 (2001).
11. B. W. Connors, M. A. Long, Annu. Rev. Neurosci. 27, 393 (2004).
12. M. V. L. Bennett, R. S. Zukin, Neuron 41, 495 (2004).
13. S. J. Cruikshank, C. E. Landisman, J. G. Mancilla, B. W. Connors, Prog. Brain Res. 149, 41 (2005).
14. G. Mitropoulou, R. Bruzzone, J. Neurosci. Res. 72, 147 (2003).
15. X. D. Yang, H. Korn, D. S. Faber, Nature 348, 542 (1990).
16. A. E. Pereda, A. Triller, H. Korn, D. S. Faber, Proc. Natl. Acad. Sci. U.S.A. 89, 12088 (1992).
17. A. Pereda et al., Proc. Natl. Acad. Sci. U.S.A. 95, 13272 (1998).
18. M. Smith, A. E. Pereda, Proc. Natl. Acad. Sci. U.S.A. 100, 4849 (2003).
19. E. M. Lasater, J. E. Dowling, Proc. Natl. Acad. Sci. U.S.A. 82, 3025 (1985).
20. M. R. Deans, B. Volgyi, D. A. Goodenough, S. A. Bloomfield, D. L. Paul, Neuron 36, 703 (2002).
21. E. C. Hampson, D. I. Vaney, R. Weiler, J. Neurosci. 12, 4911 (1992).
22. B. Rörig, G. Klausa, B. Sutor, J. Neurosci. 15, 7386 (1995).
23. P. Cobbett, G. I. Hatton, J. Neurosci. 4, 3034 (1984).
24. P. O'Donnell, A. A. Grace, J. Neurosci. 13, 3456 (1993).
25. X. D. Yang, J. A. Connor, D. S. Faber, J. Neurophysiol. 71, 1586 (1994).
26. S. H. Oliet, R. C. Malenka, R. A. Nicoll, Neuron 18, 969 (1997).
27. M. Steriade, L. Domich, G. Oakson, J. Neurosci. 6, 68 (1986).
28. M. Steriade, D. A. McCormick, T. J. Sejnowski, Science 262, 679 (1993).
29. K. H. Lee, D. A. McCormick, Neuroscience 77, 335 (1997).
30. All animal procedures were reviewed and approved by Brown University, in accordance with NIH guidelines. We thank J. Gibson for writing software, S. Patrick for technical assistance, and S. Cruikshank for helpful suggestions. Supported by NIH grants NS40528, NS25983, and NS050434 and Shore Scholars in Medicine Program, Harvard Medical School (C.E.L.).

Glial Membranes at the Node of Ranvier Prevent Neurite Outgrowth

Jeffrey K. Huang,[1,2] Greg R. Phillips,[1] Alejandro D. Roth,[3] Liliana Pedraza,[3] Weisong Shan,[3] Wiam Belkaid,[3] Sha Mi,[4] Asa Fex-Svenningsen,[5] Laurence Florens,[6] John R. Yates III,[7] David R. Colman[1,3]*

Nodes of Ranvier are regularly placed, nonmyelinated axon segments along myelinated nerves. Here we show that nodal membranes isolated from the central nervous system (CNS) of mammals restricted neurite outgrowth of cultured neurons. Proteomic analysis of these membranes revealed several inhibitors of neurite outgrowth, including the oligodendrocyte myelin glycoprotein (OMgp). In rat spinal cord, OMgp was not localized to compact myelin, as previously thought, but to oligodendroglia-like cells, whose processes converge to form a ring that completely encircles the nodes. In OMgp-null mice, CNS nodes were abnormally wide and collateral sprouting was observed. Nodal ensheathment in the CNS may stabilize the node and prevent axonal sprouting.

Myelin sheaths that wrap around neuronal axons are periodically interrupted by nodes of Ranvier that enable saltatory conduction (1) (Fig. 1A). After peripheral nervous system (PNS) injury, axonal sprouting from neighboring unlesioned nerves commonly occurs at nodes of Ranvier, allowing for the reestablishment of functional neurocircuitry (2, 3). In contrast, injury-induced sprouting rarely occurs at CNS nodes despite the absence of myelin, which is inhibitory to neurite outgrowth (4). One explanation for the nonresponsiveness of CNS axons to injury might be that sprouting is prevented by nonmyelin-derived factors present in the nodal vicinity.

To identify such inhibitory factors, we isolated membranes of the mammalian CNS nodal axoglial apparatus, comprising the node and flanking paranodal domains, by subcellular fractionation of dissected bovine, mouse, or human white matter. Because the nodal axoglial apparatus is morphologically distinct from myelin (Fig. 1B) and likely to be of greater density due to a higher protein:lipid ratio than myelin, we reasoned that membranes of the nodal axoglial apparatus might be sheared away during homogenization and be concentrated at an isopycnic density greater than that of compact myelin. We modified a synaptosome protocol (5) by using as starting material CNS white matter that contained myelinated axons and was devoid of synaptic endings. Membrane fractions were recovered from sucrose density gradients at a 0.32/1.0 M interface, comprising compact myelin membranes (6), and at a 1.0/1.25 M interface, which we provisionally termed "axogliasomes." Ultrastructural examination of axogliasomes revealed membrane profiles characteristic of paranodal loops, attached to underlying axolemmal fragments (Fig. 1C). In contrast, profiles of compact myelin and synaptosomes were rarely detected.

Immunoelectron microscopy examination with a paranode-specific marker, Caspr (7, 8), confirmed that the observed membranes were derived from the nodal axoglial apparatus (Fig. 1D). We also investigated whether axogliasomes contained appropriate biochemical markers for the nodal axoglial apparatus. The known paranodal markers Caspr, contactin, and neurofascin-155 (9), as well as the nodal marker, neurofascin-186 (10), were all detected by Western blot analysis of the axogliasome fraction, whereas compact myelin-specific markers, the proteolipid proteins PLP and DM20, were barely detected (Fig. 1E). The detection of myelin-associated glycoprotein (MAG) in compact myelin and axogliasomes was expected, because it is expressed throughout periaxolemmal channels of compact myelin and at paranodes (11). Axogliasomes are thus morphologically and biochemically distinct from membranes derived from compact myelin and comprise the entire nodal axoglial apparatus.

It is well established that purified compact myelin membranes can effectively limit neurite outgrowth activity in cell culture owing to myelin-specific inhibitory factors (4). To determine if CNS nodes of Ranvier also contain inhibitory factors for axon outgrowth,

[1]Fishberg Department of Neuroscience, Mount Sinai School of Medicine, One Gustave L. Levy Place, New York, NY 10029, USA. [2]Wellcome Trust/Cancer Research UK Gurdon Institute, University of Cambridge, Tennis Court Road, Cambridge CB2 1QR, UK. [3]The Montreal Neurological Institute, McGill University, 3801 University Street, Montreal PQ H3A 2B4, Canada. [4]Biogen Idec, Discovery Biology, 14 Cambridge Center, Cambridge, MA 02142, USA. [5]Department of Genetics and Pathology, Rudbeck Laboratory, Uppsala University, SE-751 85 Uppsala, Sweden. [6]Stowers Institute, 1000 East 50th Street, Kansas City, MO 64110, USA. [7]Department of Cell Biology SR11, The Scripps Research Institute, 10550 North Torrey Pines Road, La Jolla, CA 92037, USA.

*To whom correspondence should be addressed. E-mail: david.colman@mcgill.ca

we seeded embryonic rat cerebellar (Cb) neurons onto axogliasome-spotted culture chambers at increasing protein concentrations, and axon lengths were measured after 36 hours in culture. For comparison, we also seeded Cb neurons onto compact myelin-spotted chambers. The outgrowth capacity of Cb neurons was limited in the presence of axogliasomes, and sprouting decreased exponentially as the concentration of axogliasome proteins increased from as low as 50 ng/μl (Fig. 1F). We found that Cb neurites were on average 20 nm in length at 100 ng/μl axogliasome concentration—a near-fourfold decrease compared with control water-spotted cultures (Fig. 1H). We also found that neurite lengths decreased by nearly eightfold compared with water-spotted cultures as the concentration of axogliasomes increased up to 1000 ng/μl. Indeed, the inhibitory effect of axogliasomes on axon outgrowth was comparable to that of myelin-coated culture chambers at the same protein concentrations tested (Fig. 1, F and H). To determine if the nonpermissive effect of axogliasomes also applied to postnatal neurons, we dissected dorsal root ganglia (DRG) from postnatal day 8 (P8) rats, placed the ganglia directly onto axogliasome-coated coverslips at increasing protein concentrations, and incubated them for 7 days in culture before measuring their axon lengths. We observed the outgrowth capacity of DRG axons reduced by about fourfold, from greater than 4 mm to less than 1 mm in length, when axogliasomes concentrations increased from 25 to 1000 ng/μl (Fig. 1, G and I). These observations suggest the presence of potent inhibitory peptides at the CNS node of Ranvier that limit axon outgrowth activity in both embryonic and postnatal neurons.

To identify the protein constituents that might mediate neurite outgrowth activity, we subjected axogliasomes to proteomic analysis by multidimensional protein identification technology (MudPIT) (12). MudPIT detects peptides comprising all isoelectric points, molecular weights, and hydrophobicities, including integral membrane and low-abundance proteins. Rather than analyzing peptides derived from excised gel pieces, it separates and further fragments peptides from a solubilized membrane fraction by a combination of multidimensional liquid chromatography and tandem mass spectrometry (MS/MS), followed by an automated sequence analysis of individual peptide fragments eluted from the chromatography column. More than 300 nonredundant proteins were identified from axogliasomes (Fig. 2A), including many with known localization to the nodal axoglial apparatus (Fig. 2B). We also identified proteins that were previously unsuspected as constituents of the nodal axoglial apparatus (Fig. 2B), such as a disintegrin and metalloprotease protein 23 (ADAM23) (13), and collapsin response mediator protein 2 (Crmp-2). Several known nega-
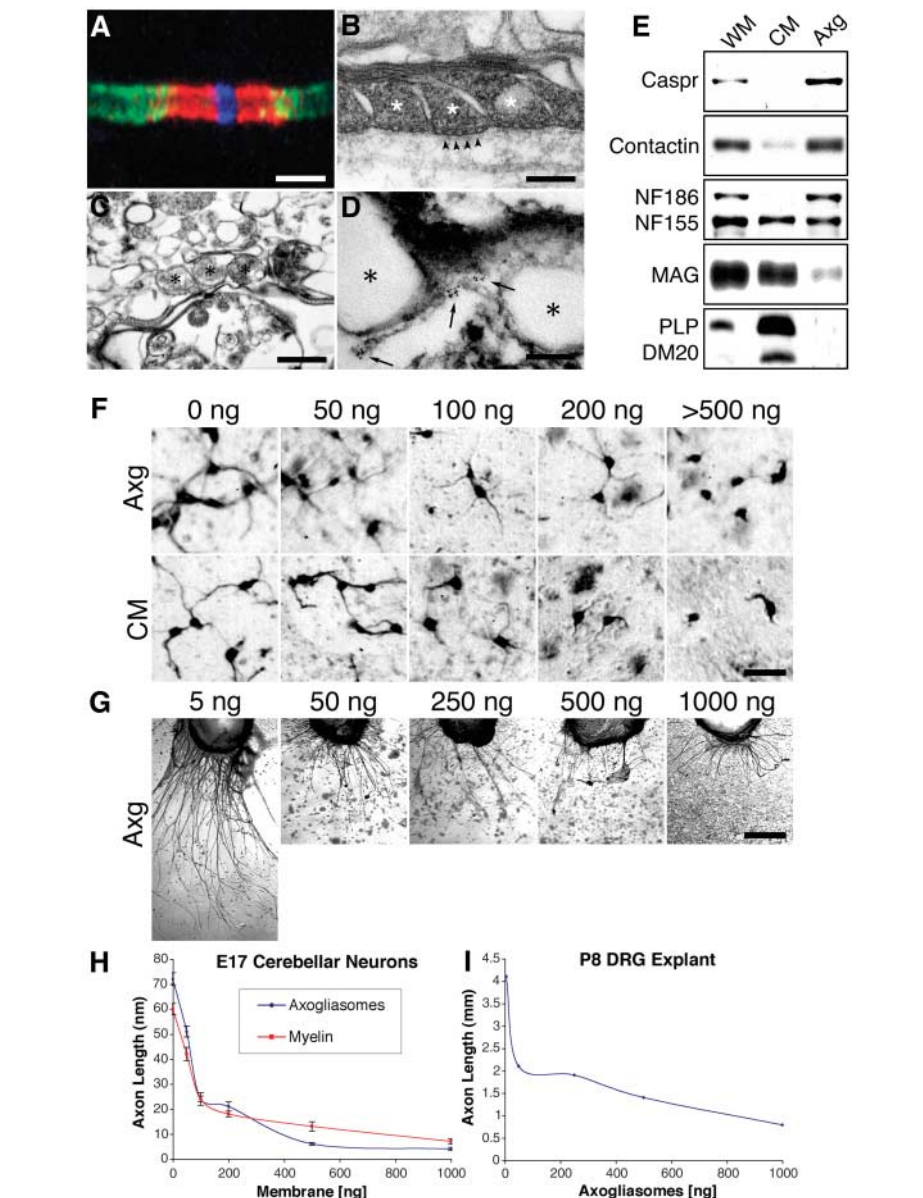

Fig. 1. Isolated membranes of CNS nodal axoglial apparatus prevent neurite outgrowth. (**A**) Longitudinal section of P15 rat spinal cord labeled with antibody to sodium channel (anti–sodium channel) (blue) at the node of Ranvier, anti-Caspr (red) at the paranode, and anti–potassium channel (green) at the juxtaparanode. Bar, 2.5 μm. (**B**) Longitudinal section of rat CNS revealed the paranode, comprising characteristic paranodal loops (asterisks) attached to the axolemma through septate densities (arrowheads). Bar, 180 nm. (**C**) Bovine axogliasomes contained 250- to 500-nm vesicles (asterisks) attached to one another and to underlying axolemmal fragments. Bar, 550 nm. (**D**) Detection of Caspr-gold particles (arrows) in isolated paranodal membranes (asterisks). Bar, 375 nm. (**E**) Western blot analysis demonstrating the enrichment of proteins from the nodal axoglial apparatus in axogliasomes (Axg) isolated from bovine white matter (WM) compared with compact myelin (CM). (**F**) At increasing mouse axogliasome (Axg) or compact myelin (CM) protein concentration, embryonic day 17 rat Cb neurite outgrowth decreases. Bar, 50 nm. (**G**) P8 rat DRG explants were cultured on axogliasome at the indicated protein concentrations. Bar, 1 mm. (**H**) Measurement of E17 rat Cb neurite outgrowth lengths under increasing Axg and CM concentrations (>50 neurites/well). Values are means ± SEM. (**I**) Measurements of mean outgrowth lengths of P8 rat DRG axons under increasing concentration of axogliasomes.

tive regulators of neurite outgrowth (Fig. 2B) were also identified, including MAG, versican, protein kinase C (14–17), and the oligodendrocyte myelin glycoprotein (OMgp) (18, 19). By Western blot analysis, OMgp was detected at the expected molecular sizes of 95 to 120 kD

(20) and was present in both CNS white matter membranes and axogliasomes (Fig. 2C).

Although its precise distribution had not been demonstrated, OMgp has generally been regarded as a component of myelin membranes (20). OMgp was not detected in compact my-
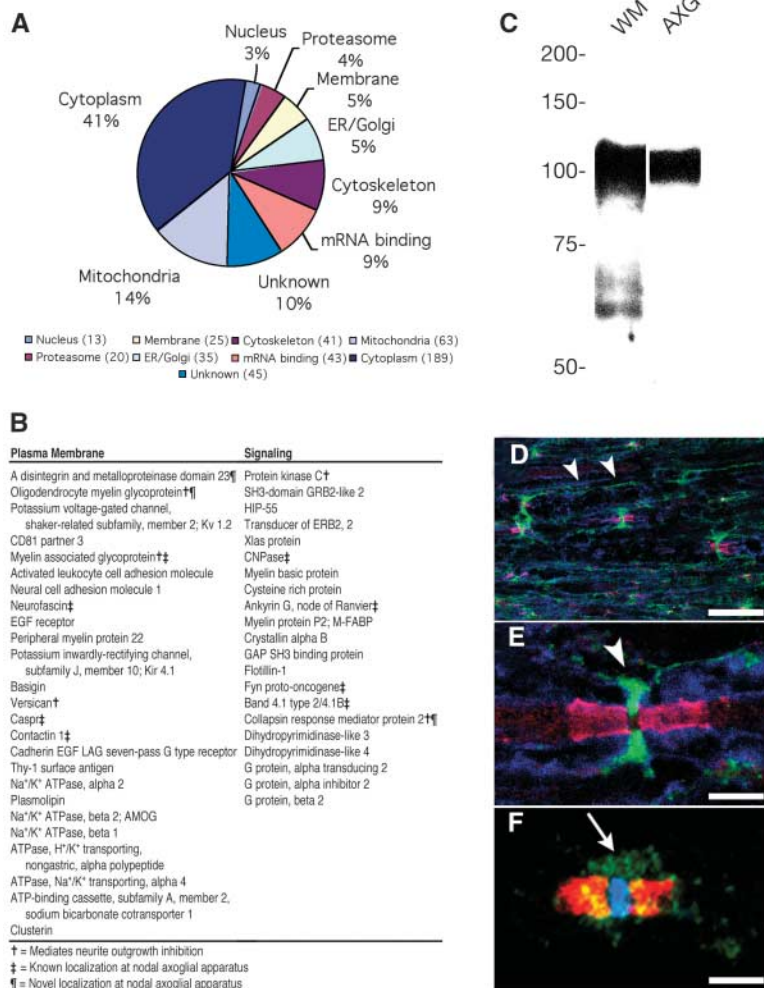
Fig. 2. Proteomic dissection of human axogliasomes reveals OMgp as a component of CNS nodal axoglial apparatus. (**A**) Functional profile of MudPIT-identified proteins. (**B**) List of candidate proteins identified from axogliasomes. (**C**) Western blot detection of OMgp at 95 to 120 kD in human white matter (WM) and axogliasomes (AXG). The lower molecular size bands detected in WM might represent degraded protein fragments, because they appear not to be present in AXG. (**D**) Longitudinally sectioned P18 rat spinal cord labeled with anti-OMgp (green) demonstrates nodal distribution. Arrowheads indicate glial processes extending on the surface of myelin before terminating at nodes of Ranvier. Paranodes were labeled with anti-Caspr (red) and compact myelin was labeled with Rip (blue). Bar, 10 μm. (**E**) At higher magnification in a sectioned P40 rat spinal cord, OMgp (green) is detected in a prominent membranous ensheathment (arrowhead) that encircles the axon at the node of Ranvier. Bar, 2 μm. (**F**) In P18 teased rat sciatic nerves, OMgp (green) was observed in PNS nerves at Schwann cell microvilli that encircle the node (arrow). Paranodes were labeled with anti-Caspr (red) and node with anti–sodium channel (blue). Bar, 2 μm.

elin in the CNS, but rather was consistently detected in thin glial membranes that appear to extend on the outer surface of myelin and terminate at nodes of Ranvier (Fig. 2D). Notably, OMgp was localized to a sharply defined, tight membranous "ring" encircling the CNS axon at the node of Ranvier (Fig. 2E). Its weak expression at the outer myelin surface resembled that of MOG, a protein component of noncompact myelin expressed in the outermost membrane (*21*) but not at the nodal locus, as we found for OMgp. OMgp was also detected at nodes of Ranvier in PNS fibers (Fig. 2F), albeit at a much lower relative labeling intensity, and in a diffuse circumnodal pattern. Its position at PNS nodes suggests that OMgp might be a

constituent of Schwann cell microvilli, which are membranous extensions of Schwann cell myelin that engage each other across the node of Ranvier. However, CNS nodes do not exhibit microvillous ensheathment and appear bare ultrastructurally (*22*); this suggested that OMgp might be expressed at CNS nodes by a different glial cell type. In transverse serial sections of a CNS nodal axoglial apparatus, we detected multiple glial processes expressing OMgp (OMgp+) that converged on and completely ensheathed the axon at the node of Ranvier (Fig. 3A, movie S1). In cerebellar cultures, we also observed OMgp+ processes in contact with developing nodes of Ranvier that flanked the elongating myelin membranes (Fig.

3C). These results suggest that OMgp is derived from a nonmyelinating glial cell type and directly interacts with a nodal component on the axon.

Previous studies have suggested the existence of astrocyte-like cells that contact the node of Ranvier (*23*, *24*). However, no convincing molecular markers for this cell type were described, and it remained unclear if these contacts were passive, or whether they were features of all CNS nodes. OMgp was not detected in conventional astrocytes, because its expression did not codistribute with the astrocyte-specific marker GFAP (glial fibrillary acidic protein) (Fig. 3F). OMgp+ cells exhibited a stellate morphology (Fig. 3, D and E) that strongly resembled that of NG2 proteoglycan-expressing (NG2+) oligodendrocyte precursor cells (OPCs) (*25*) (Fig. 3, G and H). NG2+ cells are abundantly expressed in the adult CNS, and NG2 proteoglycans have also been shown to inhibit neurite outgrowth in vitro (*25*, *26*). Like OMgp+ cells, NG2+ glial processes extended toward and encircled CNS nodes of Ranvier in the spinal cord (Fig. 3B, movie S2). It was unclear how many nodes were ensheathed by NG2+ processes because NG2 staining is most prominently detected in glial cell bodies and their processes, whereas OMgp is most prominently detected at the terminals of glial cell processes that surround the nodes of Ranvier. Although we were not able to directly demonstrate colocalization of NG2 and OMgp within the same cell with the available antisera to each protein, the observation of identical cellular morphology and the tight nodal ensheathment by NG2+ and OMgp+ glial processes, particularly in transverse spinal cord sections (Fig. 3, E and H), suggested that this is the same cell type and might represent a mature population of nonmyelinating oligodendrocytes. These cells might be similar to the recently described adult NG2+ glia that contact CNS nodes in the rat optic nerve (*27*).

The detection of OMgp+ glial processes at the node of Ranvier implies that they might participate in nodal formation and maintenance. Furthermore, the inhibitory nature of the ensheathing processes suggests that nodal ensheathment by OMgp+ cells might be necessary to prevent collateral axon outgrowth during development. To address these issues, we generated a mutant mouse lacking OMgp (OMgp−/−) by deletion of the entire coding sequence of the OMgp gene (*28*). OMgp−/− mice did not exhibit obvious behavioral abnormalities compared with the wild type at all ages examined (from P0 to P30). There also did not appear to be any changes in NG2+ cell numbers in the mutant mouse spinal cord. However, in spinal cord sections of P21 mutant mice, the axonal marker, Caspr, which sharply flanks the node in wild-type animals (Fig. 4B), was observed either in a diffuse pattern or ec-
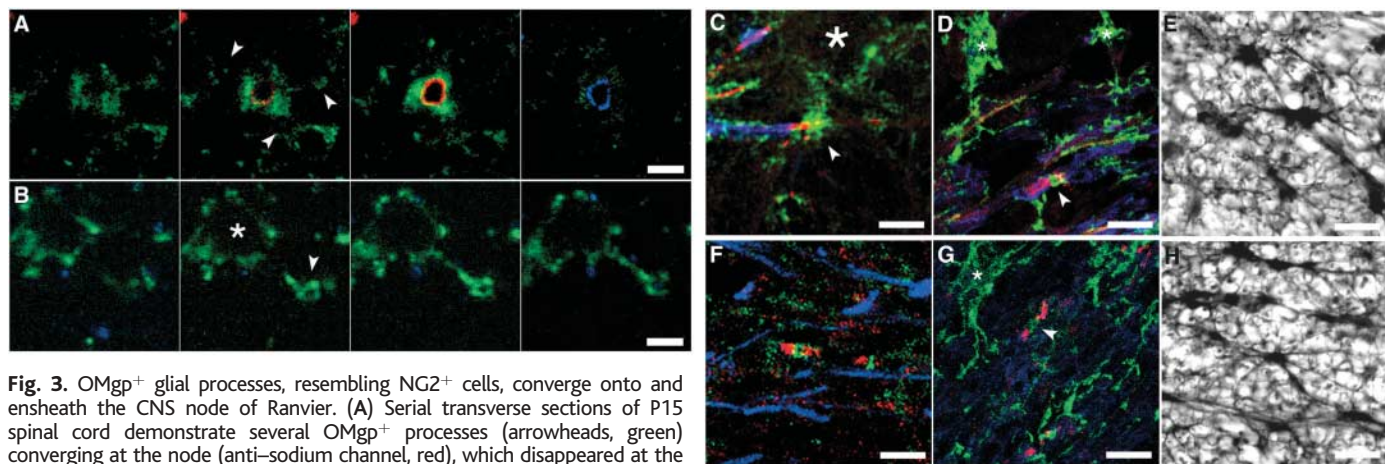
Fig. 3. OMgp+ glial processes, resembling NG2+ cells, converge onto and ensheath the CNS node of Ranvier. (**A**) Serial transverse sections of P15 spinal cord demonstrate several OMgp+ processes (arrowheads, green) converging at the node (anti–sodium channel, red), which disappeared at the paranode (anti-Caspr, blue). Bar, 2.5 μm. (**B**) An NG2+ cell (asterisk) whose process (arrowhead, green) is observed to encircle the node. Bar, 5 μm. (**C**) Immunostaining of Cb cultures demonstrates an OMgp-expressed cell (asterisk) whose process (green, arrowhead) contacts a developing hemi-node flanked by a paranode (anti-Caspr, red) and myelinating membranes (anti–myelin basic protein, blue). Bar, 7.5 μm. (**D**) P15 rat spinal cord revealed OMgp+ glial cells (asterisks, green) resembling oligodendrocyte precursor cells. Arrowhead points to a node. Bar, 7.5 μm. (**E**) Immunoper- oxidase labeling of P18 spinal cord transverse section demonstrates abundant OMgp+ cells with stellate morphology. Bar, 15 μm. (**F**) GFAP (blue) expressed by astrocytes do not colocalize with OMgp (green). Bar, 5 μm. (**G**) An oligodendrocyte precursor-like cell (asterisk, green) labeled with anti-NG2 proteoglycan. NG2+ processes were observed to contact the node (arrowhead). Bar, 8 μm. (**H**) NG2+ cells resemble the OMgp+ stellate cells. Bar, 14 μm.
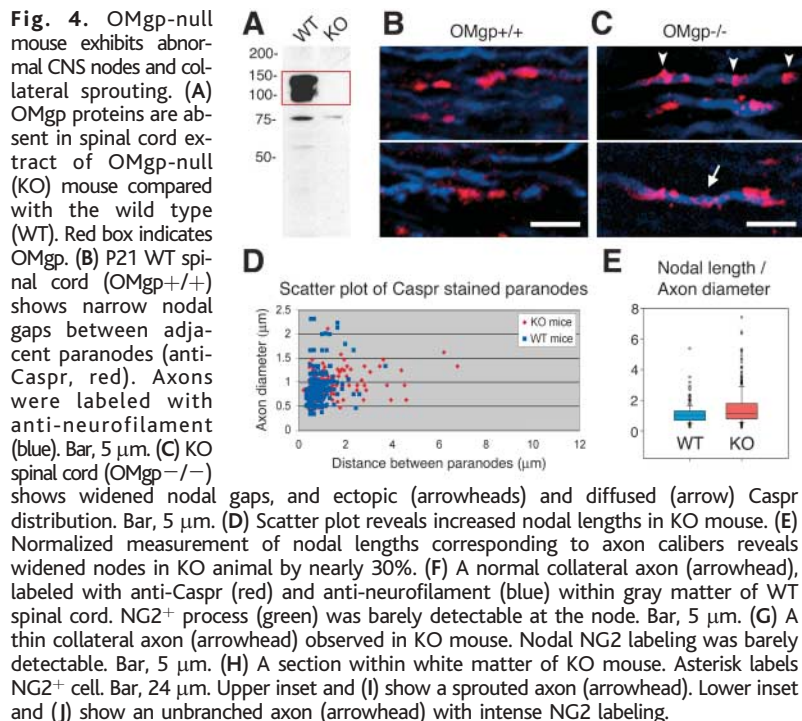

Fig. 4. OMgp-null mouse exhibits abnormal CNS nodes and collateral sprouting. (**A**) OMgp proteins are absent in spinal cord extract of OMgp-null (KO) mouse compared with the wild type (WT). Red box indicates OMgp. (**B**) P21 WT spinal cord (OMgp+/+) shows narrow nodal gaps between adjacent paranodes (anti-Caspr, red). Axons were labeled with anti-neurofilament (blue). Bar, 5 μm. (**C**) KO spinal cord (OMgp−/−) shows widened nodal gaps, and ectopic (arrowheads) and diffused (arrow) Caspr distribution. Bar, 5 μm. (**D**) Scatter plot reveals increased nodal lengths in KO mouse. (**E**) Normalized measurement of nodal lengths corresponding to axon calibers reveals widened nodes in KO animal by nearly 30%. (**F**) A normal collateral axon (arrowhead), labeled with anti-Caspr (red) and anti-neurofilament (blue) within gray matter of WT spinal cord. NG2+ process (green) was barely detectable at the node. Bar, 5 μm. (**G**) A thin collateral axon (arrowhead) observed in KO mouse. Nodal NG2 labeling was barely detectable. Bar, 5 μm. (**H**) A section within white matter of KO mouse. Asterisk labels NG2+ cell. Bar, 24 μm. Upper inset and (**I**) show a sprouted axon (arrowhead). Lower inset and (**J**) show an unbranched axon (arrowhead) with intense NG2 labeling.

topically clustered on the axon (Fig. 4C). Indeed, nodal lengths, which are ~0.5 to 1 μm in normal mice, were much more variable in mutant mice, ranging from ~0.5 to 7 μm (Fig. 4D). Because nodal sizes may vary owing to differences in axon caliber, we calculated the ratio of measured nodal lengths to measured axon diameters and found that on average, nodal length was ~30% greater in the mutant than in wild-type animals (Fig. 4E). These observations indicate that the establishment of CNS nodes is impaired in OMgp-null mice and

that OMgp is likely required for this process to proceed at a normal pace.

Several discrete axons sprouting from nodes of Ranvier were observed in OMgp-null mice in both gray (Fig. 4G) and white matter regions (Fig. 4, H and I). At least 30 nodal sprouts were detected in 10 mutant mouse spinal cord sections. These bifurcated axons exhibited wider nodal gaps and abnormal Caspr labeling, suggesting that the loss of OMgp might enable collateral sprouting. We also observed, but with lower frequency, occasional

collateral sprouting in gray and white matter regions of wild-type spinal cord, in which we detected 12 sprouts from 10 examined spinal cord sections (Fig. 4F). These are likely normally branched axons; in these cases, nodal gaps and Caspr staining appeared no different from unbranched axons. It is extremely unlikely that the observed sprouted axons in OMgp-null mice were the result of nearby axons crossing at the node, because we inspected each of the individually collected confocal laser scanned slices (at 0.1 μm per slice) from

all imaged spinal cord sections to rule out possible axon intersections. Notably, in all of the collaterally sprouted axons from both mutant and wild-type animals, NG2+ glial processes were barely detectable at the nodal vicinity (Fig. 4I), whereas many nonsprouted nodes appeared to be in contact with NG2+ glial processes (Fig. 4J). This observation further indicates that nodal ensheathment is necessary to prevent axonal sprouting.

In conclusion, we find that isolated membranes of CNS nodes of Ranvier are nonpermissive for neurite outgrowth and propose that this is due to cell extensions that emanate from NG2+ oligodendrocyte precursor-like cells that tightly ensheath the nodal axon. It is known that NG2 is expressed by a heterogeneous population of neuroglial cells in the adult CNS, ranging from oligodendrocyte precursors to specialized glial cells that contact nodes of Ranvier in optic nerves and synaptic terminals in the hippocampus (29–31). Whether these nodal glial cells represent the same lineage of specialized NG2+ neuroglia described to contact nodes of Ranvier in rat optic nerves remains to be determined. Furthermore, we found glial processes emanating from specialized oligodendrocyte-like cells that converge at the CNS node and contain high concentrations of the neurite outgrowth inhibitor, OMgp. OMgp was detected at most of the nodes examined, which suggests that it may function in generating normal nodal architecture and in suppressing collateral sprouting, because in OMgp-null mice, the nodal gap is abnormally widened and sprouting from this locus is observed. It also remains to be determined whether OMgp is necessary for survival of the NG2+ oligodendrocyte precursor-like cells, although given the lack of decrease in NG2+ cells in the OMgp$^{-/-}$ mice, this may not be a likely functional role for OMgp. It seems more likely that OMgp plays a role in the adhesion of NG2+ glial processes to CNS nodes because in all of the observed sprouted nodes, there were no detectable NG2+ processes.

Finally, considering the intimate relation between the node and the encircling inhibitory glial membranes, after traumatic injury to the CNS, OMgp and possibly other inhibitory peptides at the nodal/paranodal region, such as versican, MAG, NG2, or Nogo-A (11, 16, 27, 32), may remain stably attached to the nodal region or become deposited on the axonal surface, thus preventing axons from responding to injury-elicited growth signals. Overcoming the inhibitory nature of these nodal glial cells may yield new therapeutic interventions to promote functional recovery after CNS trauma.

References and Notes

1. L. Pedraza, J. K. Huang, D. R. Colman, *Neuron* **30**, 335 (2001).
2. J. R. Slack, W. G. Hopkins, M. N. Williams, *Nature* **282**, 506 (1979).
3. Q. T. Nguyen, J. R. Sanes, J. W. Lichtman, *Nat. Neurosci.* **5**, 861 (2002).
4. M. E. Schwab, P. Caroni, *J. Neurosci.* **8**, 2381 (1988).
5. G. R. Phillips *et al.*, *Neuron* **32**, 63 (2001).
6. W. T. Norton, S. E. Poduslo, *J. Neurochem.* **21**, 749 (1973).
7. S. Einheber *et al.*, *J. Cell Biol.* **139**, 1495 (1997).
8. M. Menegoz *et al.*, *Neuron* **19**, 319 (1997).
9. S. Tait *et al.*, *J. Cell Biol.* **150**, 657 (2000).
10. S. Lambert, J. Q. Davis, V. Bennett, *J. Neurosci.* **17**, 7025 (1997).
11. U. Bartsch, F. Kirchhoff, M. Schachner, *J. Comp. Neurol.* **284**, 451 (1989).
12. M. P. Washburn, D. Wolters, J. R. Yates III, *Nat. Biotechnol.* **19**, 242 (2001).
13. A. P. Goldsmith, S. J. Gossage, C. ffrench-Constant, *J. Neurosci. Res.* **78**, 647 (2004).
14. G. Mukhopadhyay, P. Doherty, F. S. Walsh, P. R. Crocker, M. T. Filbin, *Neuron* **13**, 757 (1994).
15. B. P. Niederost, D. R. Zimmermann, M. E. Schwab, C. E. Bandtlow, *J. Neurosci.* **19**, 8979 (1999).
16. T. Oohashi *et al.*, *Mol. Cell. Neurosci.* **19**, 43 (2002).
17. R. Sivasankaran *et al.*, *Nat. Neurosci.* **7**, 261 (2004).
18. V. Kottis *et al.*, *J. Neurochem.* **82**, 1566 (2002).
19. K. C. Wang *et al.*, *Nature* **417**, 941 (2002).
20. D. D. Mikol, K. Stefansson, *J. Cell Biol.* **106**, 1273 (1988).
21. C. Brunner, H. Lassmann, T. V. Waehneldt, J. M. Matthieu, C. Linington, *J. Neurochem.* **52**, 296 (1989).
22. A. Peters, S. Palay, H. Webster, *The Fine Structure of the Nervous System* (Oxford Univ. Press, New York, ed. 3, 1991).
23. R. H. Miller, B. P. Fulton, M. C. Raff, *Eur. J. Neurosci.* **1**, 172 (1989).
24. C. ffrench-Constant, R. H. Miller, J. Kruse, M. Schachner, M. C. Raff, *J. Cell Biol.* **102**, 844 (1986).
25. J. M. Levine, J. P. Card, *J. Neurosci.* **7**, 2711 (1987).
26. C. L. Dou, J. M. Levine, *J. Neurosci.* **14**, 7616 (1994).
27. A. M. Butt *et al.*, *Glia* **26**, 84 (1999).
28. D. Mikol *et al.*, *J. Cell Biol.* **111**, 2673 (1990).
29. D. E. Bergles, J. D. Roberts, P. Somogyi, C. E. Jahr, *Nature* **405**, 187 (2000).
30. M. Berry, P. Hubbard, A. M. Butt, *J. Neurocytol.* **31**, 457 (2002).
31. J. M. Levine, R. Reynolds, J. W. Fawcett, *Trends Neurosci.* **24**, 39 (2001).
32. D. Y. Nie *et al.*, *EMBO J.* **22**, 5666 (2003).
33. We thank D. Mikol, P. Brophy, and G. Gennarini for providing antibodies, and members of the D.R.C. lab for helpful suggestions. This work was supported by grants from the Canadian Institutes of Health Research and the NIH (NS20147), the National Multiple Sclerosis Society (RG 3217-A-8), the Myelin Repair Foundation, and the New York State Spinal Cord Injury Trust (NYS CO17683) to D.R.C. J.R.Y. was supported by NIH grant P41 RR11823.

The Widespread Impact of Mammalian MicroRNAs on mRNA Repression and Evolution

Kyle Kai-How Farh,[1]* Andrew Grimson,[1]* Calvin Jan,[1] Benjamin P. Lewis,[1,2] Wendy K. Johnston,[1] Lee P. Lim,[3] Christopher B. Burge,[2] David P. Bartel[1]†

Thousands of mammalian messenger RNAs are under selective pressure to maintain 7-nucleotide sites matching microRNAs (miRNAs). We found that these conserved targets are often highly expressed at developmental stages before miRNA expression and that their levels tend to fall as the miRNA that targets them begins to accumulate. Nonconserved sites, which outnumber the conserved sites 10 to 1, also mediate repression. As a consequence, genes preferentially expressed at the same time and place as a miRNA have evolved to selectively avoid sites matching the miRNA. This phenomenon of selective avoidance extends to thousands of genes and enables spatial and temporal specificities of miRNAs to be revealed by finding tissues and developmental stages in which messages with corresponding sites are expressed at lower levels.

MicroRNAs are an abundant class of endogenous ~22-nucleotide (nt) RNAs that specify posttranscriptional gene repression by base-pairing to the messages of protein-coding genes (1, 2). Hundreds of miRNAs have been identified in humans (1), and thousands of messages are under selection to maintain pairing to miRNA seeds (nucleotides 2 to 7 of the miRNA), enabling regulatory targets of miRNAs to be predicted simply by searching 3′ untranslated regions (3′UTRs) for evolutionarily conserved 7-nt matches to miRNA seed regions (3–5).

We used the mouse expression atlas (6) to examine the expression of the predicted targets of six tissue-specific miRNAs: miR-1 and miR-133 (skeletal muscle), miR-9 and

[1]Whitehead Institute for Biomedical Research, Department of Biology, Massachusetts Institute of Technology, and Howard Hughes Medical Institute, 9 Cambridge Center, Cambridge, MA 02142, USA. [2]Department of Biology, Massachusetts Institute of Technology, Cambridge, MA 02139, USA. [3]Rosetta Inpharmatics, 401 Terry Avenue North, Seattle, WA 98109, USA.

*These authors contributed equally to this work.
†To whom correspondence should be addressed. E-mail: dbartel@wi.mit.edu